Biochimica et Biophysica Acta 1850 (2015) 1215–1223

Contents lists available at ScienceDirect

Biochimica et Biophysica Acta

journal homepage: www.elsevier.com/locate/bbagen

$Na_v1.5$ channels can reach the plasma membrane through distinct *N*-glycosylation states

Aurélie Mercier [a], Romain Clément [a], Thomas Harnois [a,b], Nicolas Bourmeyster [a,b], Patrick Bois [a], Aurélien Chatelier [a,*]

[a] *Laboratoire Signalisation et Transports Ioniques Membranaires (STIM), ERL CNRS 7368, Université de Poitiers, Pôle Biologie Santé, Bâtiment B36, 1 rue Georges Bonnet, TSA 51106, 86073 Poitiers Cedex 9, France*

[b] *CHU de Poitiers, 1 rue de la Milétrie, 86021 Poitiers CEDEX, France*

ARTICLE INFO

Article history:
Received 16 June 2014
Received in revised form 26 January 2015
Accepted 16 February 2015
Available online 23 February 2015

Keywords:
Voltage-gated sodium channel
$Na_v1.5$
N-glycosylation
Secretory pathway
Negative dominance
Brugada syndrome

ABSTRACT

Background: Like many voltage-gated sodium channels, the cardiac isoform $Na_v1.5$ is well known as a glycoprotein which necessarily undergoes *N*-glycosylation processing during its transit to the plasma membrane. In some cardiac disorders, especially the Brugada syndrome (BrS), mutations in $Na_v1.5$ encoding gene lead to intracellular retention and consequently trafficking defect of these proteins. We used two BrS mutants as tools to clarify both $Na_v1.5$ glycosylation states and associated secretory behaviors.

Methods: Patch-clamp recordings and surface biotinylation assays of HEK293T cells expressing wild-type (WT) and/or mutant $Na_v1.5$ proteins were performed to assess the impact of mutant co-expression on the membrane activity and localization of WT channels. Enzymatic deglycosylation assays and brefeldin A (BFA) treatments were also employed to further characterize recombinant and native $Na_v1.5$ maturation.

Results: The present data demonstrate that $Na_v1.5$ channels mainly exist as two differentially glycosylated forms. We reveal that dominant negative effects induced by BrS mutants upon WT channel current result from the abnormal surface expression of the fully-glycosylated forms exclusively. Furthermore, we show that core-glycosylated channels can be found at the surface membrane of BFA-treated or untreated cells, but obviously without generating any sodium current.

Conclusions: Our findings provide evidence that native and recombinant $Na_v1.5$ subunits are expressed as two distinct matured forms. Fully-glycosylated state of $Na_v1.5$ seems to determine its functionality whereas core-glycosylated forms might be transported to the plasma membrane through an unconventional Golgi-independent secretory route.

General significance: This work highlights that *N*-linked glycosylation processing would be critical for $Na_v1.5$ membrane trafficking and function.

1. Introduction

$Na_v1.5$ channels represent one of the nine functionally pore-forming α-subunits ($Na_v1.1$–$Na_v1.9$) constituting the voltage-gated sodium channel (VGSC) family [1]. Each Na_v channel exists as multimeric complexes presumably composed of one α-subunit and one or several regulatory $Na_v\beta$-subunits ($Na_v\beta1$–$Na_v\beta4$) [2,3]. As the predominant cardiac VGSC isoform, $Na_v1.5$ channels play a key role in cardiac excitability and conduction as carrying large inward depolarizing sodium currents responsible for cardiac action potential initiation. During their biosynthetic trafficking, these transmembrane proteins are subject to extensive post-translational modifications like phosphorylations [4–8], methylations [9,10] as well as glycosylations [11–13].

VGSC α isoforms are assumed to be heavily glycosylated proteins containing approximately 20–30% by weight of carbohydrates [14–16]. Interestingly, $Na_v1.5$ channels might be considered as an exception since only 5% of their mature mass could be attributed to *N*-linked oligosaccharides [11]. The post-translational *N*-glycosylation of nascent Na_v channels would be initiated in the endoplasmic reticulum (ER). Sialic acid residues which account for 40% of Na_v complex carbohydrates [15,17] are thought to be subsequently transferred to acceptor oligosaccharides, presumably into the *trans*-Golgi subcompartment.

Previous reports indicated that *N*-glycans and particularly capping sialic acids could modulate the gating of different Na_v channels, including the cardiac isoform [12,13,16,18,19]. However, the presence of these residues does not seem to be not required for their proper membrane

Abbreviations: BFA, Brefeldin A; BrS, Brugada syndrome; Endo H, endoglycosidase H; ER, endoplasmic reticulum; HEK, human embryonic kidney cells; HMW, high-molecular weight; LMW, low-molecular weigh; PNGase, peptide *N*-glycosidase F; VGSC, voltage-gated sodium channel; WT, wild-type

* Corresponding author at: ERL CNRS 7368, Université de Poitiers, UFR SFA, Pôle Biologie Santé, Bâtiment B36/B37, 1 rue Georges Bonnet, TSA 51106, 86073 POITIERS Cedex 9, France. Tel.: +33 5 49 45 37 47; fax: +33 5 49 45 40 14.

E-mail address: aurelien.chatelier@univ-poitiers.fr (A. Chatelier).

http://dx.doi.org/10.1016/j.bbagen.2015.02.009
0304-4165/

expression in native cardiac tissues [20]. Intriguingly, the modulation of $Na_v1.7$ membrane expression and resulting sodium current density was shown to be glycosylation-dependent [21]. Moreover, the completion of *N*-glycosylation process would be essential for proper membrane localization of other voltage-gated channels like potassium and more recently calcium channels [22–26]. Thus, studying the impact of *N*-glycosylation modifications in channel folding, trafficking and function allows to refine the understanding of the regulation of membrane excitability.

Several previous studies have already highlighted the existence of a negative dominance observed for $Na_v1.5$ mutants found in Brugada syndrome (BrS) patients over WT channels [27–31]. All findings suggest that this deleterious impact would be correlated with an alteration of wild-type (WT) channel trafficking. However, to date, the underlying causes and the fate of retained WT proteins remain unknown. The present study was initiated to provide a comprehensive understanding of membrane $Na_v1.5$ transport and maturation in the context of physiological or pathological situations such as BrS.

2. Experimental procedures

2.1. Genetic constructs

Co-transfection conditions involved the use of several plasmid vectors encoding WT or mutant $Na_v1.5$ channels and their auxiliary β_1-subunit. The cloning of the full length SCN5A/WT and SCN5A/R1432G into pcDNA vectors was described previously [32]. The cDNA encoding SCN5A/L325R subcloned in the plasmid pcDNA3 was a generous gift of Dr. Hugues Abriel (University of Bern, Bern, Switzerland). The human sodium channel $Na_v\beta1$-subunit and CD8 were constructed in pIRES bicistronic vector (pCD8-IRES-β_1).

2.2. Cell culture, transfection and treatments

Human embryonic kidney (HEK) 293T cells were grown in Dulbecco's modified Eagle's medium (DMEM, BioWhittaker) containing 10% fetal bovine serum (Biowest), 100 μg/mL streptomycin and 100 U/mL penicillin (Gibco). In parallel, a stable cell line expressing $Na_v1.5$ (kindly provided by Prof. Mohamed Chahine, Laval University, QC, Canada) was maintained using identical culture conditions.

Plasmid constructs were transiently transfected into HEK293T cells using the calcium phosphate method as detailed in our previous study [31]. For biochemical and patch-clamp experiments, each transfection condition was adjusted to include 2.4 μg of DNA per 60 mm dish with HEK cells at 30% confluence. Transfection conditions were mimicking either monoallelic states (WT/(−), (−)/L325R, (−)/R1432G; with 0.6 μg SCN5A plasmids and 0.6 μg empty vectors) or patient heterozygosity (WT/L325R, WT/R1432G; with equivalent amounts (0.6 μg) of WT and mutant SCN5A constructs).

In indicated experiments and immediately after transfection, HEK293T cells were incubated with 50 to 500 ng/mL brefeldin A (LC Laboratories) or with ethanol vehicle at 37°C for 24 or 48 h before cell lysis or patch-clamp recordings.

For protein glycosylation inhibition, transfected cells were also treated in culture with tunicamycin (Sigma-Aldrich) for 18 h at varying concentrations (0.2, 0.5 or 1 μg/mL).

2.3. Protein extraction

Stably and transiently transfected cells were washed with cold PBS and lysed by scraping the cells into lysis buffer (10 mM Tris, 1% Nonidet P-40, 0.5% deoxycholic acid) supplemented with protease inhibitor cocktail (Sigma-Aldrich). Cell lysates were then incubated for 30 min on ice and centrifuged at 20,000*g* for 5 min at 4 °C.

An alternative protocol was applied for the solubilization of cardiac tissue proteins. Human right atrial biopsies were removed during heart bypass surgery procedures as previously described [33–35]. All procedures were performed in accordance with the Declaration of Helsinki. Each biopsy was cut into small pieces in lysis buffer and then incubated under rotation at 4°C for 2 h. Samples were ground with a tissue grinder, and centrifuged at 250*g* during 5 min to remove tissue fragments. The homogenates were cleared by centrifugation at 20,000*g* for 10 min prior to determine protein contents in the supernatants.

Protein contents were measured using DC protein assay (Biorad) with BSA as a reference. Cleared cell lysates were denatured in 2× sample buffer (126 mM Tris HCl, 20% glycerol, 4% SDS and 0.02% bromophenol blue, pH 6.8) containing 5% 1-thioglycerol (Sigma-Aldrich) for 60 min at 37°C.

2.4. Deglycosylation assays

For deglycosylation experiments, peptide *N*-glycosidase F (PNGase F, cat. G5166, Sigma-Aldrich) and endoglycosidase H (Endo H, cat. 11 088 726 001, Roche Applied science) were used according to the manufacturer's instructions with some modifications.

Total cell lysates from transfected HEK293T cells (125 μg) or from cardiac biopsies (225 μg) were heated at 37°C for 30 min in denaturating phosphate buffer (0.1% SDS, 0.05% β-mercaptoethanol, 7 mM KH_2PO_4, 43 mM Na_2HPO_4, pH 7.5). After cooling on ice, denaturated proteins were supplemented first with 0.15% Triton X-100 and then with either 5 units of PNGase F or equivalent volume of phosphate buffer. Samples were finally incubated at 37°C for 5 h before denaturation step in 2× sample buffer and SDS-PAGE analysis.

For Endo H enzymatic assays, same protein lysate amounts were previously placed in denaturating sodium buffer (0.1% SDS, 0.05% β-mercaptoethanol, 10 mM $C_2H_3NaO_2$, 5 mM EDTA, 0.2% Nonidet P-40, pH 5.5) and then 100 milliunits of Endo H or sodium buffer were added to achieve similar final volumes. Enzymatic reactions were carried out as described for PNGase treatments.

2.5. Cell surface biotinylation

Biotinylation experiments were carried out on transfected HEK293T cells grown at 80–90% confluence in 60-mm dishes.

Forty-eight hours post-transfection, the cells were washed twice with ice-cold PBS (Phosphate Buffered Saline: 137 mM NaCl, 1.5 mM KH_2PO_4, 2.7 mM KCl and 8 mM Na_2HPO_4, pH 7.4) and once with PBS containing 0.5 mM $CaCl_2$ and 1 mM $MgCl_2$, pH 8 (PBSCM). Plates were incubated with 0.5 mg/mL EZ-Link Sulfo-NHS-SS-Biotin (Pierce) freshly diluted in PBSCM for 30 min at 4°C. The biotinylation reaction was ended by washing the cells three times 5 min with PBSCM containing 50 mM glycine and 5 mg/mL BSA. After three PBS washes, cells were scraped in lysis buffer containing protease inhibitor cocktail (Sigma). Cell lysates were then incubated on ice for 30 min and clarified at 20,000*g* for 5 min at 4°C. Biotinylated proteins were isolated by incubating overnight cleared lysates (100 μg of proteins) with 15 μL of streptavidin-agarose resins (Pierce) at 4°C in lysis buffer. Beads were pelleted by centrifugation and washed three times with NET buffer (50 mM Tris, 150 mM NaCl, 5 mM EDTA and 0.05% Nonidet P-40, pH 7.4). Biotinylated cell surface proteins were eluted at 37°C for 60 min in 15 μL of 2 × sample buffer containing 5% 1-Thioglycerol (Sigma). Total cell lysates and biotinylated proteins were subjected to SDS-PAGE before immunoblotting analysis as described below.

2.6. Immunoblotting

Proteins from biotinylated samples and cell lysates were separated by SDS-PAGE using 5% polyacrylamide gels and transferred to 0.45 μm nitrocellulose sheets. Membranes were blocked 1 h in TBS-Tween blocking solution (100 mM Tris–HCl, 150 mM NaCl and 0.1% Tween-20, pH 7.6) with 5% nonfat dry milk and then probed overnight at 4 °C with primary antibodies rabbit polyclonal SP19 anti-pan-Na_v (1:1000, Alomone Labs),

mouse anti-Na^+/K^+-ATPase α1 subunit (1:1000, Santa Cruz), mouse monoclonal anti-β-actin (1:10,000, Sigma) or mouse anti-Ezrin (1:250, BD Transduction Laboratories). Membranes were washed and incubated for 1 h at room temperature with anti-rabbit or anti-mouse horseradish peroxidase-conjugated secondary antibodies (1:10,000, Interchim). Membranes were washed with TBS-Tween and revealed with ECL chemiluminescent substrate (GE Healthcare). For biotinylation assays, signal intensities of bands in the immunoblots were quantified using Scion image analysis software (Scion Corp). After background subtraction, a rectangular region of interest was set to include one or both signals corresponding to distinct $Na_v1.5$ glycosylated products. For each transfection condition, surface $Na_v1.5$ density value was then normalized to the corresponding total "two bands" $Na_v1.5$ density.

2.7. Patch clamp recordings

HEK293T cells were used for electrophysiology assays 48 h post-transfection and 24 h after plating by trypsinization into 35-mm dishes. Sodium currents were recorded in the whole-cell patch-clamp configuration as previously described [31].

Briefly, whole-cell currents were filtered at 5 kHz and acquired at 100 kHz using an Axopatch 200A amplifier (Molecular Devices) and Clampex 10.2 acquisition software (Molecular Devices). Low-resistance pipettes (1.5–2 MΩ) were pulled from borosilicate glass capillary tubes (GC150T-10, Harvard Apparatus) and coated with HIPEC® R6101 (Dow Corning, Midland, MI, USA). Pipette solution contained (35 mM NaCl, 105 mM CsF, 10 mM EGTA and 10 mM HEPES, pH adjusted to 7.4 with CsOH). The bath solution had the following composition: (60 mM NaCl, 2 mM KCl, 1.5 mM $CaCl_2$, 1 mM $MgCl_2$, 10 mM glucose, 10 mM HEPES and 90 mM CsCl, pH adjusted to 7.4 with NaOH). The liquid junction potential of 4 mV was corrected prior to experiments. Capacity transients were canceled and voltage errors were minimized using 80% series resistance compensation. Leak-subtracted (P/4) sodium currents were evoked from a holding potential of −140 mV using 50-ms depolarizing steps from −100 to 30 mV in 10-mV increments every 5 s. Current density-voltage relationships were determined by normalizing the peak currents to cell capacitance (pA/pF) plotted versus the applied voltage.

2.8. Data analysis and statistics

Data were analyzed using Clampfit 10.2 (Molecular Devices), Origin 8.0 (Microcal Software), and Microsoft Excel. Statistical analyses were performed with Student *t*-test or one-way analysis of variance (ANOVA) with Bonferroni's post hoc tests for multiple mean comparisons using Origin 8.0 (Microcal Software, Inc.). Differences were considered statistically significant at p values <0.05. Results were reported as mean ± SEM for the number of observations indicated.

3. Results

3.1. Distinct mutations on $Na_v1.5$ extracellular loops alter WT sodium current densities

We began our study by reproducing the heterozygosity of Brugada patients carriers of two specific $Na_v1.5$ mutations that were partially characterized [29,31,32,36]. The L325R and R1432G mutations display the particularity to occur within distinct extracellular S5–S6 loops of the $Na_v1.5$ α subunit, into DI and DIII domains respectively. A similar strategy used in our previous work for the R1432G mutant [31] was reiterated to assess the influence of L325R channels on the WT proteins. Transient transfections were carried out to express either WT (WT/(−)) or mutant channels alone ((−)/L325R; (−)/R1432G) or both WT and mutant together (WT/L325R; WT/R1432G) in HEK293T cells. Whole-cell current recordings were then performed. All considered conditions presented typical $Na_v1.5$ sodium currents and current voltage relationships with an activation that began at a potential of approximately −80 mV and a peak current density observed at ~ −40 mV (Fig. 1A & B).

When L325R was expressed alone ((−)/L325R), transfected cells displayed a small peak current density of 71.2 ± 8.9 pA/pF (n = 9) equal to 21% of mean current density measured in WT/(−) condition (n = 12, Fig. 1B and C). As expected, this mutant induced a clear dominant negative effect when co-expressed with WT channels. Indeed, WT/L325R conditions induced a significant reduction of 40% in membrane current density (196.2 ± 29.4 pA/pF, n = 9) compared to WT/(−) (327.6 ± 23.0 pA/pF, n = 12, $P < 0.01$, *t*-test) (Fig. 1C).

For experiments involving R1432G expression, we have already shown that the mutant R1432G expressed alone ((−)/R1432G, n = 7) did not produce any membrane current while its co-expression significantly reduced the WT current density by 65% in comparison with WT/(-) condition (n = 11, $p < 0.01$, *t*-test) (Fig. 1C) [31].

Based on all these results, we clearly demonstrate the occurrence of a strong dominant negative effect of both R1432G and L325R upon total membrane current density when co-expressed with the WT protein in our cell model.

3.2. Dominant negative effect is associated with the alteration of $Na_v1.5$ maturation pattern

The luminometric surface assay have already been carried out to establish a link between the functional dominant-negative R1432G mutant and the disruption of WT channel trafficking [31]. To further analyze the impact of L325R and R1432G mutants on $Na_v1.5$ expression, we next investigated the level of surface protein expression using the surface biotinylation technique.

Immunoblots illustrated in Fig. 2A show total and surface $Na_v1.5$ expression observed in total cell lysates and biotinylated protein fractions, respectively. In order to ensure that the biotinylation reflects the specific labeling of proteins expressed at the membrane, immunoblots were also probed with anti-ezrin antibody which specifically binds to an intracellular protein. As expected, no ezrin signal was detected in biotinylated fractions compared to positive immunoblot observed for total lysate (Fig. 2A).

First, it is particularly interesting to note that total $Na_v1.5$ expression patterns seem similar among all transfection conditions, except for (−)/L325R which is characterized by a drastic reduction of the upper band intensity (Fig. 2A). As for the biotinylated protein fraction, $Na_v1.5$ mutants expressed either alone or with WT forms exhibit broadly reduced signal intensities compared to WT channels. To estimate $Na_v1.5$ membrane expression levels, surface/total ratios were then calculated using densitometric analysis of the two major bands (Fig. 2A, green and purple arrows) observed at approximately 250 kDa (Fig. 2B). Expression of WT, mutant or combined forms did not significantly modify $Na_v1.5$ amount at the cell surface, except for (-)/R1432G where it was reduced by 53% compared with WT/(−) ($P < 0.01$, ANOVA).

However, because the $Na_v1.5$ signal is composed of two bands which presumably correspond to distinct maturation states, we re-analyzed biotinylation immunoblots by discriminating each form of $Na_v1.5$ (Fig. 2C and D).

Interestingly, we obtained significant differences in membrane expression level of the high-molecular weight (HMW) channels between the tested transfection conditions (Fig. 2C). Expression of L325R or R1432G mutants alone resulted in a significant reduction of membrane HMW forms by respectively 61% and 90% compared with WT/(−) condition ($P < 0.001$, ANOVA). When WT and mutant channels were co-expressed, this expression level was reduced to 56% and 54% of WT/(−) for WT/L325R and WT/R1432G ($P < 0.05$, ANOVA). By contrast, no significant variation in membrane low-molecular weight (LMW) form expression was detected between all conditions (Fig. 2D).

The observed decrease in the amount of membrane HMW channels could result either from a trafficking defect of this particular form or from a decreased intracellular maturation process. As noted above, except for (−)/L325R condition, the densitometric analysis of the expression

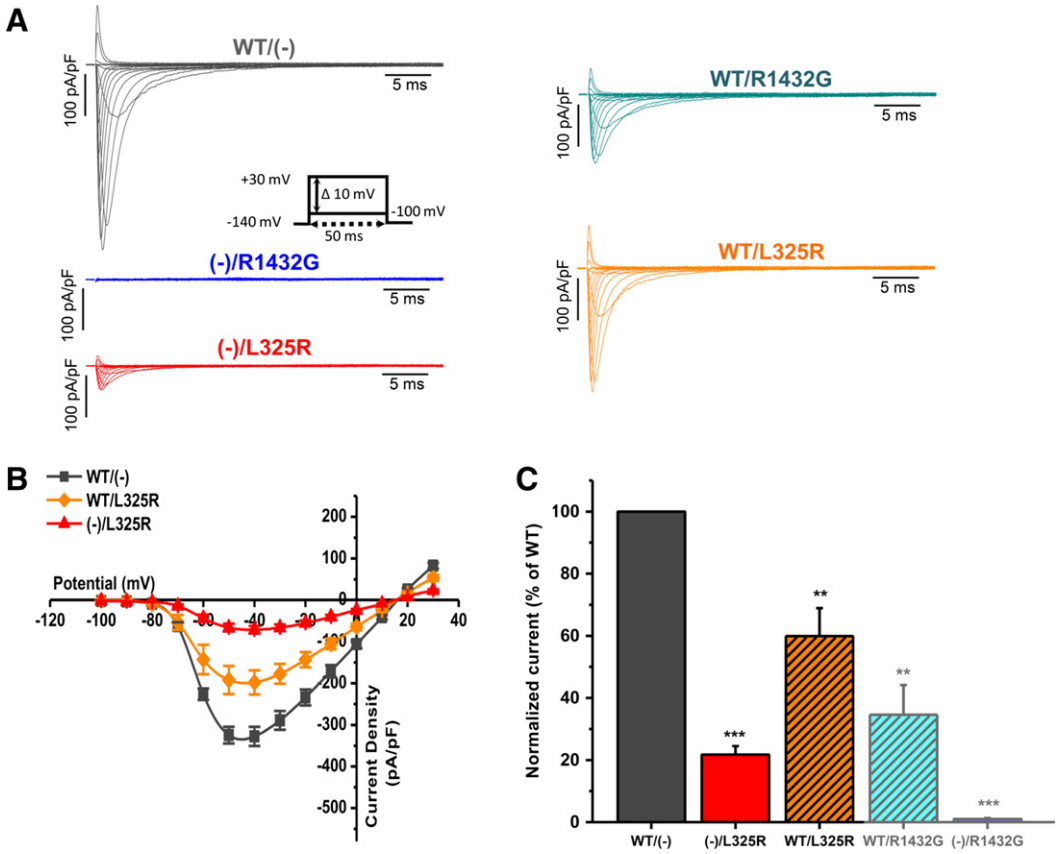

Fig. 1. Distinct $Na_v1.5$ mutants exhibit similar dominant negative effects upon WT sodium current. (A) Representative whole-cell recordings were shown for HEK2 93T cells expressing WT and/or mutant channels. Heterozygous transfection conditions consisted in expressing WT channels with empty vector (WT/(−)), WT and mutant channels (WT/R1432G; WT/L325R) or mutant channels with empty vector ((−)/R1432G); (−)/L325R). Sodium current traces were obtained using the voltage-clamp protocol shown in the inset and are presented as membrane current densities. (B) Peak current–voltage relationships of $Na_v1.5$ currents recorded from 9–12 cells using the protocol as shown in Fig. 1A. Only transfection and co-transfection data with L325R mutant are reported here. (C) Average peak current densities of WT and/or mutant channels were measured at −40 mV and then normalized to the WT/(−) condition. It should be noted that experiments using R1432G mutant were already published by our group in Mercier et al., 2012. Statistical analyses were carried out independently for each mutant versus the corresponding WT/(−) condition. **, $P < 0.01$; ***, $P < 0.001$ *vs* WT/(−) condition (Student *t*-test).

level of HMW $Na_v1.5$ did not reveal any statistical variation between all total protein fractions (data not shown). In the specific case of L325R mutant, HMW protein amount was shown to be limited in both total and surface membrane fractions. As a consequence, the differences in membrane HMW $Na_v1.5$ expression were not directly correlated to maturation defect of the proteins.

Our results indicate that dominant-negative effects of both mutants on WT channels result in reduced cell surface expression of HMW forms exclusively.

3.3. $Na_v1.5$ exhibits two major glycosylated states in vivo and in vitro

Next, because the $Na_v1.5$ signal is characterized by the presence of these two particular bands, we further studied the nature of this double-band signal.

First of all, in order to ensure that this characteristic was not related to our heterologous expression system, $Na_v1.5$ protein expression pattern was compared between transiently and stably transfected HEK293T cells and native human cardiac biopsies (Fig. 3A).

Theoretically, the 4.2-kb cDNA used for transfections encodes a protein of 2016 amino acids, with a calculated molecular weight of 227 kDa [37]. However, the present results show that $Na_v1.5$ channels are expressed as distinct forms with molecular weights exceeding 250 kDa (Fig. 3A). Indeed, immunoblots revealed the presence of two bands named A and B which migrated at 270 and 250 kDa respectively. Interestingly, these two matured forms were found to exist in both HEK293T cells and native tissue models. It should be specified that the signal intensity ratio of A-band to B-band was found to be inverted between HEK293T cells and cardiac biopsies as determined by densitometric measurements (0.4 ± 0.1 *vs* 4.5 ± 1.2, $n = 3$, $p < 0.05$, *t*-test). The difference observed between these immunoreactive channels and the predicted molecular weight $Na_v1.5$ is probably due to posttranslational modifications conferring them their final maturation state.

N-linked glycosylation sites present on human $Na_v1.5$ polypeptide (GenBank accession number M77235) was predicted using the NetNGlyc 1.0 server (http://www.cbs.dtu.dk/services/NetNGlyc). Only Asn-Xaa-Ser/Thr motifs (where Xaa denotes any amino acid except proline) located on extracellular loops and with a prediction score superior to 0.5 were withheld as putative *N*-glycosylation sites (Fig. 3B) [38]. It should be noted that L325R substitution occurred on the edge of four clustered potential glycosylation sequences and might prevent mutant $Na_v1.5$ maturation. Indeed, contrary to R1432G and WT channels, L325R protein pattern exhibits a unique Na_v signal band in total fraction (Fig. 2A). This intriguing observation led us to investigate the two main maturation states of $Na_v1.5$ channels (bands A and B, in Fig. 3A).

First, tunicamycin, an antibiotic blocking oligosaccharide synthesis, was used to prevent *N*-glycosylation process of nascent polypeptide chains at an early stage [39]. Tunicamycin treatment was applied in culture to HEK293T cells expressing WT $Na_v1.5$ channels at increasing concentrations from 0.2 to 1 μg/mL for 18 h (Fig. 3C). Interestingly, the lowest concentration of tunicamycin was sufficient to eliminate Na_v B-band and to diminish A-band intensity. In addition, the use of higher concentrations of tunicamycin resulted in abolishing the A- and B-band signals, but also in producing non-glycosylated forms (~230 kDa) of $Na_v1.5$ channels.

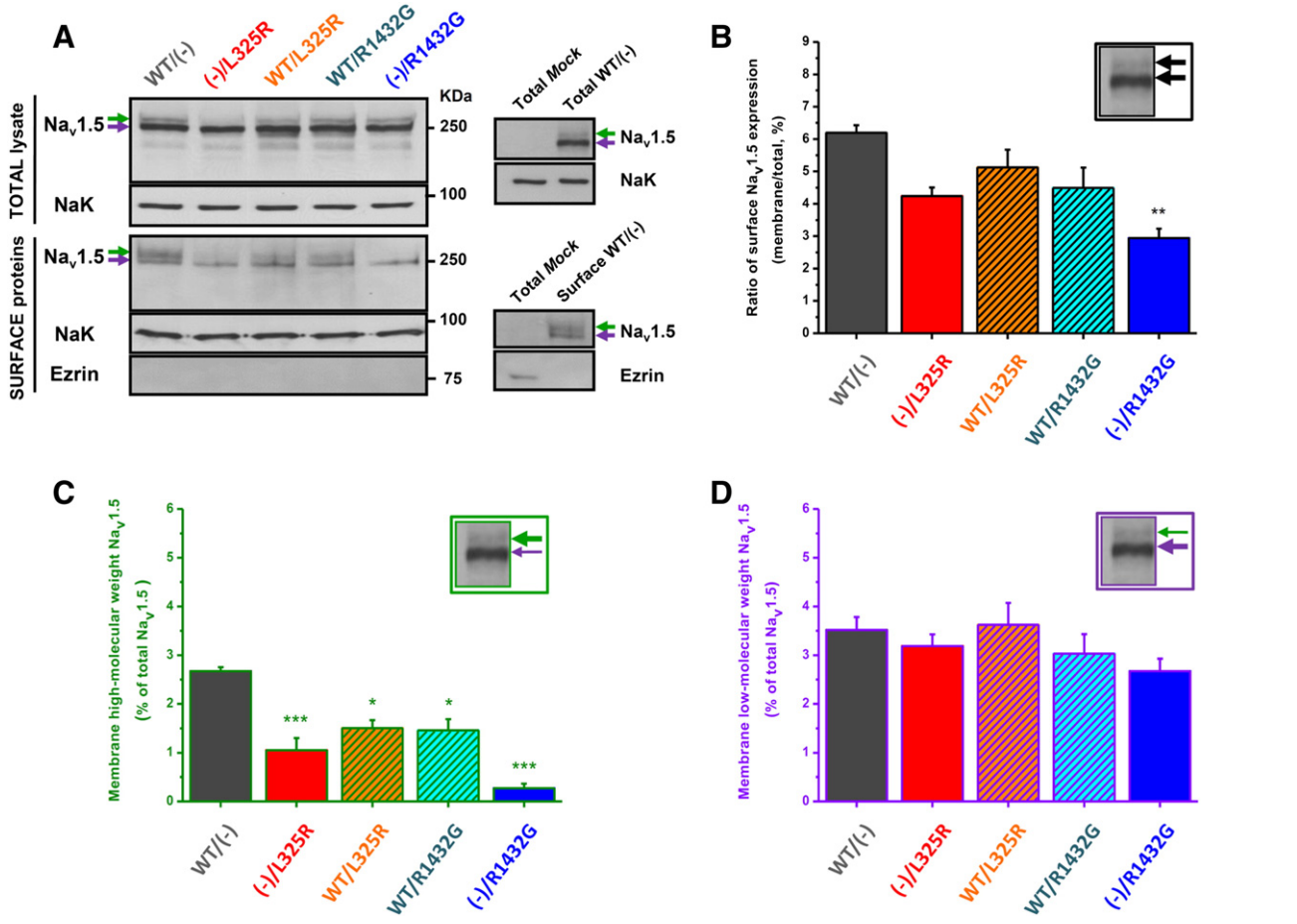

Fig. 2. Influence of the co-expression of WT and mutant channels on their global and plasma membrane expressions. (A) Representative western blots of total and surface-biotinylated proteins from HEK293T cells transfected with WT channels and empty vector (WT/(−)), WT and mutant channels (WT/R1432G; WT/L325R), mutant channels and empty vector ((−)/R1432G; (−)/L235R) or with empty vector alone (Mock). Total cell lysates (10 μg for each condition) and biotinylated membrane proteins were separated on 5% SDS-PAGE gels and probed with anti-pan-Na$_v$ antibody (Na$_v$1.5) and anti-Na^+/K^+ ATPase α1 subunit antibody (NaK) as a positive membrane protein marker. Ezrin antibody was used as a negative control. Colored arrows indicate the bands corresponding to high- (green) and low- (purple) molecular weight Na$_v$1.5 channels. (B) Quantification of relative density values of Na$_v$1.5 signals obtained from immunoblots. The relative ratio of surface expression to total amount of Na$_v$1.5 channels was estimated by dividing the biotinylated signal by corresponding total Na$_v$1.5 signal. As biotinylated proteins were purified from 100 μg of total lysates but only 10 μg were loaded, all ratio values were finally multiplied by 0.1 to reflect actual surface channel proportions. Data were plotted as the means and errors of three independent experiments (**, $P < 0.01$ compared with WT/(−) condition; ANOVA). (C and D) Alternative quantifications of the ratio of membrane High- (C) and Low-molecular weight fractions (D) to total Na$_v$1.5 expression from biotinylation immunoblots. Data were expressed as percentage of total Na$_v$1.5 signal (***, $P < 0.001$; **, $P < 0.01$; *, $P < 0.05$ compared with WT/(−) condition; ANOVA).

As the two distinct A and B maturation forms seem to be modified by *N*-glycosylation, we further investigated the heterogeneity of attached *N*-glycans. Two different enzymatic deglycosylation strategies were employed on several protein lysates from transfected HEK293T cells and human cardiac tissues (Fig. 3D). PNGase F was used to equally release high-mannose, hybrid and complex *N*-glycans from Na$_v$1.5 proteins whereas only high-mannose type oligosaccharides could be specifically cleavable by Endo H. Typically, Na$_v$1.5 sensitivity to these different enzymes would allow to discriminate between the ER-localized channels modified by high-mannose sugars (PNGase and Endo H sensitive) and those which have undergone post-*cis*-Golgi maturation (PNGase sensitive and Endo H resistant). Our results showed a shift in the migration of the two Na$_v$1.5 bands in PNGase F-treated lysates compared to untreated protein samples from both heterologous expression systems and native tissues (Fig. 3D, upper immunoblots). Indeed, PNGase F treatment reduced these immunoreactive bands that were converted into a single ~235-kDa deglycosylated band (red arrow). Concerning the Endo H deglycosylation assays (Fig. 3D, lower immunoblots), the B-band was found to be sensitive to enzymatic digestion in all treated lysates contrary to the A-band which appeared broadly unaffected. Note that only the HMW subunits (A-band), which are largely expressed in cardiac atrial tissues, could be examined under our experimental conditions.

Taken together, these findings suggest that native as well as recombinant Na$_v$1.5 subunits are expressed as two differentially *N*-glycosylated forms. The LMW channels (B-band) would acquire an "immature" glycosylation state typical for ER compartment, whereas the A-form could be considered as the mature form of Na$_v$1.5 modified with complex oligosaccharide chains.

3.4. Na$_v$1.5 channels may reach the plasma membrane via the classical and an unconventional pathway

We therefore examined the link existing between the glycosylation modifications of Na$_v$1.5 channels and their membrane transport through the secretory pathway. To this end, cell treatment with the fungal metabolite brefeldin A (BFA) was used as a common strategy to block classical membrane protein trafficking without interfering with unconventional secretory routes [40].

In our experimental conditions, HEK293T cells were simultaneously transfected with WT sodium channels and incubated with 50 or 500 ng/mL BFA during 24 to 48 h. Na$_v$1.5 maturation states and their sensitivity to BFA-treatment were then monitored by analyzing total and membrane protein fractions and whole-cell sodium current density (Fig. 4).

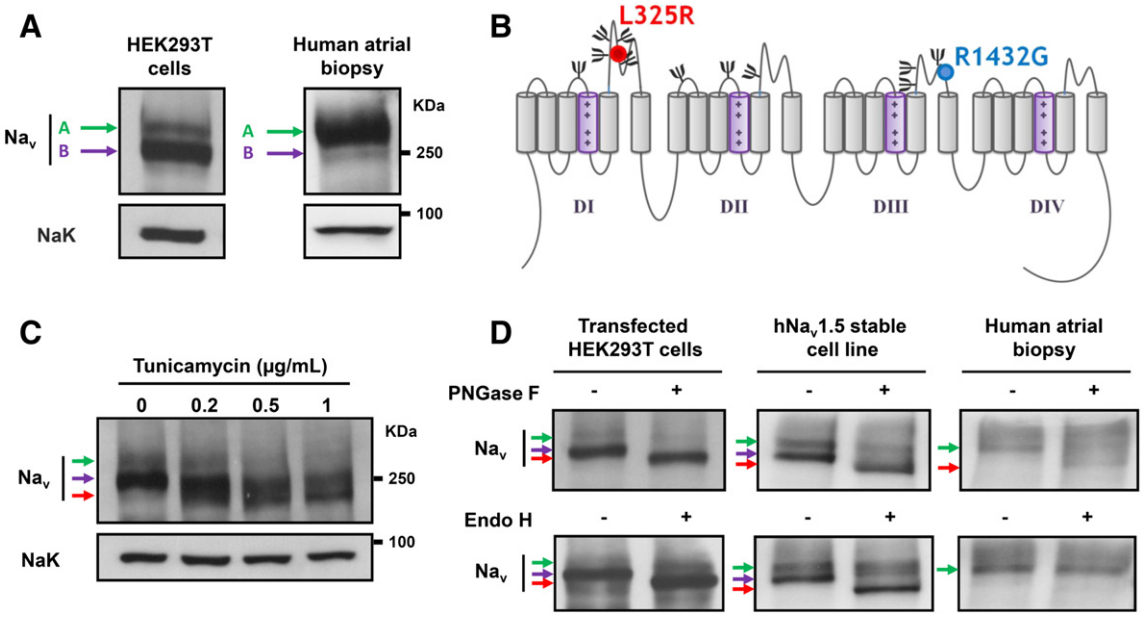

Fig. 3. The two major $Na_v1.5$ forms are differentially *N*-glycosylated. (A) Comparative expression patterns of WT Na_v channels expressed in HEK293T cell line and native cardiac tissues. Whole cell extracts of transfected HEK293T cells (15 μg) and human atrial biopsies (100 μg) were separated by 5% SDS-polyacrylamide gel electrophoresis, blotted and probed with rabbit polyclonal anti-pan sodium channel (top) and mouse monoclonal anti-Na/K-ATPase α1 (bottom). The two distinguishable forms (A and B) of the $Na_v1.5$ α-subunit are indicated with arrows. (B) Membrane topology of $Na_v1.5$ channels and relative positions of L325R and R1432G mutations. The 11 putative *N*-glycosylation sites, determined by the NetNGlyc 1.0 algorithm, are indicated with treelike structures (ψ). (C) Prevention of $Na_v1.5$ *N*-glycosylation. Representative western blot showing the effect of treatment with tunicamycin. HEK293T cells expressing WT $Na_v1.5$ channels were incubated with 0.2, 0.5 or 1 μg/mL tunicamycin or with DMSO vehicle for 18 h. The red arrow indicates the bands corresponding to non-glycosylated channels. (D) Deglycosylation assays of Na_v channels with endoglycosidase treatments. Digestions were performed using cell lysates of transiently or stably transfected HEK293T cells ($n = 3$) and from human atrial tissues. Protein samples were treated (+) or not (−) with peptide *N*-glycosidase F (PNGase F) and endoglycosidase H (Endo H) prior to gel electrophoresis and immunoblotting.

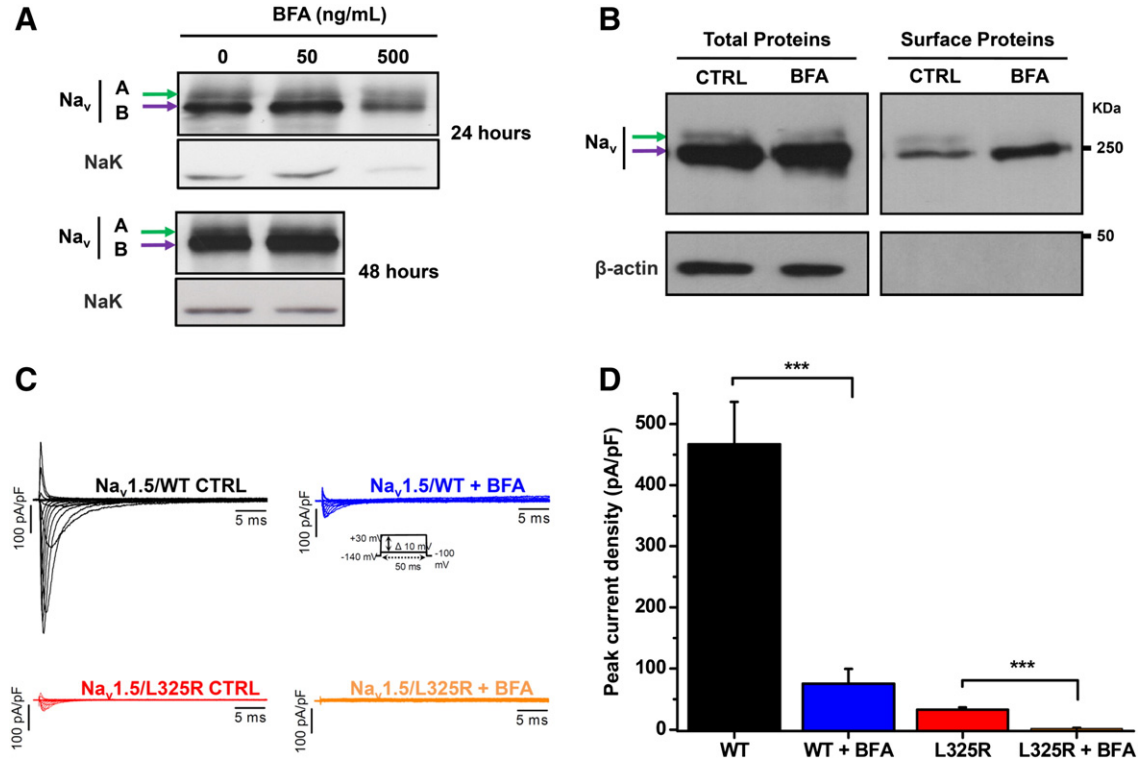

Fig. 4. Effects of Brefeldin A on WT $Na_v1.5$ expression, membrane transport and current density. (A) Representative western blots showing the effects of treatment with brefeldin A (BFA at 50 or 500 ng/mL for 24 or 48 h) on HEK293T cells transiently expressing WT $Na_v1.5$ channels. The main $Na_v1.5$ forms are indicated with arrows. (B) Representative immunoblot of three independent experiments showing total and membrane biotinylated $Na_v1.5$ channels. Cell lysates were obtained from transfected cells incubated with 50 ng/mL brefeldin A (BFA) or ethanol (CTRL) for 48 h. To ensure that biotin labeling of membrane proteins was specific to the cell membrane surface, β-actin was used as a negative intracellular marker. (C) Representative whole-cell current traces of HEK293T cells transiently expressing WT and L325R $Na_v1.5$ channels and previously treated with BFA 50 ng/mL or vehicle (CTRL) for 48 h. Current amplitudes were elicited from a holding membrane potential of −140 mV to various test potentials (see inset) and then normalized to cell capacitance. (D) Statistical analysis of peak current densities obtained at −40 mV from whole-cell recordings in BFA-treated and control transfected HEK293T cells. ***, $p < 0.001$ ($n = 6$, student *t*-test).

Our first finding revealed that both HMW and LMW $Na_v1.5$ channels remained unaffected after BFA treatment for all tested concentrations and incubation durations (Fig. 4A). However, more interestingly, surface biotinylation assays show a specific BFA-mediated impact on the HMW matured forms (Fig. 4B). In fact, the B-band signals corresponding to the membrane LMW proteins seems to be unaffected in BFA-treated condition ($p = 0.79$; *t*-test) whereas in contrast, the surface amount of HMW channels were found to be reduced to 44% of control condition ($p < 0.05$; *t*-test). This latter observation must be related to the functional alteration of sodium current measured in cells upon BFA incubation for 48 h at 50 ng/mL (Fig. 4C and D). Indeed, whole-cell mean current density recorded in BFA-treated transfected cells (75.4 ± 23.9 pA/pF, $n = 6$) was significantly reduced by 84% compared to control cells (466.6 ± 69.5 pA/pF; $n = 6$, $P < 0.001$, *t*-test). BFA-treatment was reiterated on L325R/$Na_v1.5$-expressing cells and was found to fully abolish Na + currents observed in control conditions (2.0 ± 1.0 pA/pF *vs* $32,5 \pm 3.8$ pA/pF recorded from untreated cells, $n = 6$, $P < 0.01$, *t*-test).

Finally, our findings suggest that (i) the LMW $Na_v1.5$ proteins would be early *N*-glycosylated channels generated in the ER that could reach the plasma membrane through an unconventional Golgi-independent pathway, (ii) the BFA-sensitive HMW forms could represent the mature and functional channels which traffic to the cell surface via the classical secretory transport route.

4. Discussion

4.1. BrS negative dominance as result of $Na_v1.5$ late trafficking disruption?

This study provides new insights into the maturation states of native and recombinant $Na_v1.5$ channels which mainly exist as two differentially glycosylated forms. As illustrated in Fig. 5, these proteins can be modified by sequential *N*-glycan addition and processing during their transit through the ER and Golgi apparatus. Interestingly, we show that both fully and partially glycosylated channels are expressed at the plasma membrane in HEK293T cells.

However, in this work, we demonstrate that the negative dominance of both R1432G and L325R mutants occurs through an alteration in the secretory membrane traffic of the HMW WT proteins exclusively. Furthermore, our findings suggest that the attached *N*-glycans on these particular forms would undergo terminal maturation into late Golgi compartment. Previous studies by our group and others have demonstrated the occurrence of cardiac α–α subunit interactions underlying the deleterious impact of BrS $Na_v1.5$ mutations on WT channels [30,31,41]. Accordingly, the biotinylation experiments strongly suggest that this α–α physical association would be downstream of the terminal maturation process although this does not preclude an earlier interaction mechanism between $Na_v1.5$ channels. Intriguingly, $Na_v1.5$ α-subunit oligomerization has shown to be modulated by $Na_v\beta$ subunits. Indeed, we previously showed that α–α interactions would only occur in the presence of $Na_v\beta1$ subunits whereas another recent study reported that $Na_v\beta3$ subunits could form trimeric clusters also including $Na_v1.5$ subunits [31,42]. Interestingly, these two auxiliary subunits were found as differentially modulating *N*-glycosylation of another sodium channel isoform $Na_v1.7$ [21]. As a consequence, strong consideration should be given to further investigation for their regulatory role in Na_v maturation and trafficking.

4.2. Co-existence of two distinct pools of membrane $Na_v1.5$: what about their activities?

As *N*-linked glycosylations affect and promote the proper folding of nascent polypeptide chains [43], our study was oriented to address the functional significance of each maturation state of $Na_v1.5$ channels.

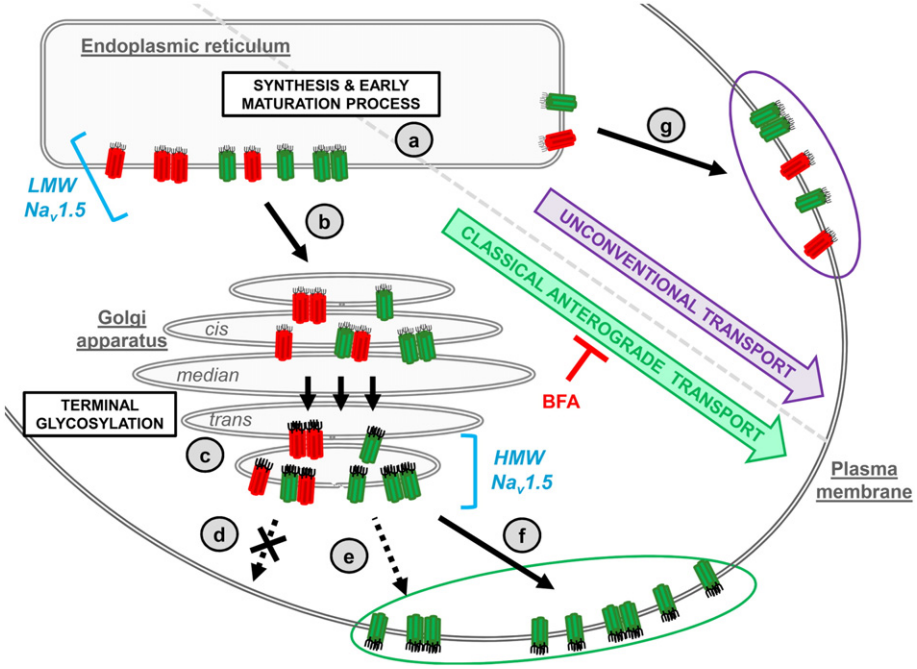

Fig. 5. Hypothetical model of the maturation and the trafficking of $Na_v1.5$ mutants and wild-type (WT) proteins. After their synthesis, $Na_v1.5$ channels are located into the endoplasmic reticulum (ER) where the first *N*-glycosylation step (a) is completed, producing low-molecular weight (LMW) $Na_v1.5$ mutant (red) and WT (green) proteins. Afterward, LMW glycosylated channels are transported to the Golgi apparatus in which attached *N*-glycans could be further trimmed and modified (c), this terminal glycosylation process conferring a resistance to Endo-H digestion. Then, WT and mutant $Na_v1.5$ channels may have multiple fates depending on the cellular expression context. While the membrane transport of the HMW mutant channels is entirely abolished (d), these proteins can still exert a dominant negative effect on the terminal trafficking of equivalent WT forms (e). This results in reduced surface localization of $Na_v1.5$ channels compared to cells exclusively expressing WT proteins (f). Alternatively, both WT and mutant channels are also found at the cell surface in their low-molecular weight (LMW) forms. Indeed, after reaching an "immature" glycosylated state in the ER, these channels could use a BFA-insensitive trafficking pathway (g). Note that although our experimental conditions included the co-expression of the regulatory subunit $Na_v\beta1$, its potential involvement in the trafficking, the maturation or the physical association of α-subunits is not illustrated here.

Patch-clamp and biochemical results indicate that both studied mutants, especially non-functional R1432G channels, are present at the plasma membrane but only in their LMW forms. Intriguingly, as small currents were recorded from L325R $Na_v1.5$ expressing cells we suggest that a minority of HMW mutants could reach efficiently the surface membrane but obviously would remain undetectable under our biotinylation experiments. The alteration of total and surface HMW L325R channels could be explained either by the ER retention of these mutants downstream of final *N*-glycosylation process or by the direct disruption of this maturation step. Thus, discrepancies between R1432G and L325R expression patterns would imply that fully-glycosylated state might not be sufficient to proper $Na_v1.5$ surface membrane expression. In addition, the BFA-induced reduction of WT sodium current densities is associated with the loss of membrane HMW channels exclusively. Thus, it seems reasonable to postulate that immature LMW $Na_v1.5$ proteins are totally non-functional. Moreover, the abolition of the current observed when L325R/$Na_v1.5$-expressing cells were treated with BFA confirmed the hypothesis that in control conditions, a limited amount of HMW forms should reach the plasma membrane and support the small currents recorded. However, this hypothesis contrasts with previous studies which suggest the inability of *N*-glycans to affect VGSC functionality, although *N*-glycosylations would be required for their surface transport or even could influence their stability and their gating [13,44,45]. One possibility would be that early *N*-glycosylation would be sufficient for cell surface trafficking of $Na_v1.5$ channels, although extensive trimming and remodeling of their *N*-glycans and/or additional posttranslational maturations into Golgi compartments appear to be required for the channel functionality. Therefore, it would be of great interest to identify the *N*-glycan structures found in the two LMW and HMW channels. This is particularly essential considering that $Na_v1.5$ proteins are differentially glycosylated depending on the cardiac chamber and the considered developmental stage [12,46].

4.3. Evidence for a novel unconventional route for immature $Na_v1.5$ channels

An important and interesting insight provided by our study concerns the differential sensitivity of LMW and HMW forms to BFA treatment. While the fully-glycosylated channels seem to be typically transported through the classical Golgi-mediated pathway, a pool of immature forms that have not undergone their terminal maturation could also travel to the plasma membrane via an unconventional route (Fig. 5). Although the underlying secretory mechanisms remain to be characterized for VGSC, it should be mentioned that such alternative Golgi-independent targeting has already been reported for other ion channels like K_v4 voltage-gated potassium channels or the cystic fibrosis transmembrane conductance regulator [47–49]. These previous results are consistent with the existence of multiple early secretory routes that could ensure the ER escape and then the membrane transport of native core-glycosylated $Na_v1.5$ proteins. However, further studies are needed to prove that this alternative anterograde protein flow is not directly linked to our cell model but could also exist in native tissues under physiological or pathological conditions. If that was the case, this export pathway would potentially be used for the clearance of accumulating proteins in the ER and may represent a constitutive response to relieve or to prevent ER stress. However, in pathological conditions, accumulation of non-functional proteins to the plasma membrane would also be problematic for membrane organization and function.

In summary our results raise questions about the role of *N*-glycosylations on $Na_v1.5$ channels. Although much remains to be done including the identification of sugar attachment sites and oligosaccharide structures, the present study suggests that these posttranslational modifications could not be limited to track $Na_v1.5$ progression through the secretory pathway. In addition to contribute to their functionality, *N*-glycans might be crucial for controlling $Na_v1.5$ folding, trafficking and maybe their membrane stability. As a consequence, additional work in native tissues would be required to address the involvement of *N*-glycosylation in the cellular fate of VGSC.

Transparency document

The Transparency document associated with this article can be found, in the online version.

Acknowledgements

This work was supported by CNRS and Ministère de l'Education Nationale, de l'Enseignement Supérieur et de la Recherche. We would like to thank Dr. Jean-Claude Hervé for critical reading and comments of the manuscript.

References

[1] W.A. Catterall, A.L. Goldin, S.G. Waxman, International Union of Pharmacology. XLVII. Nomenclature and structure-function relationships of voltage-gated sodium channels, Pharmacol. Rev. 57 (2005) 397–409.
[2] W.A. Catterall, From ionic currents to molecular mechanisms: the structure and function of voltage-gated sodium channels, Neuron 26 (2000) 13–25.
[3] G.A. Patino, L.L. Isom, Electrophysiology and beyond: multiple roles of Na + channel beta subunits in development and disease, Neurosci. Lett. 486 (2010) 53–59.
[4] H. Hallaq, D.W. Wang, J.D. Kunic, A.L. George Jr., K.S. Wells, K.T. Murray, Activation of protein kinase C alters the intracellular distribution and mobility of cardiac Na + channels, Am. J. Physiol. Heart Circ. Physiol. 302 (2012) H782–H789.
[5] C.A. Ahern, J.F. Zhang, M.J. Wookalis, R. Horn, Modulation of the cardiac sodium channel NaV1.5 by Fyn, a Src family tyrosine kinase, Circ. Res. 96 (2005) 991–998.
[6] J. Zhou, H.G. Shin, J. Yi, W. Shen, C.P. Williams, K.T. Murray, Phosphorylation and putative ER retention signals are required for protein kinase A-mediated potentiation of cardiac sodium current, Circ. Res. 91 (2002) 540–546.
[7] N.M. Ashpole, A.W. Herren, K.S. Ginsburg, J.D. Brogan, D.E. Johnson, T.R. Cummins, D.M. Bers, A. Hudmon, Ca2 +/calmodulin-dependent protein kinase II (CaMKII) regulates cardiac sodium channel NaV1.5 gating by multiple phosphorylation sites, J. Biol. Chem. 287 (2012) 19856–19869.
[8] C. Marionneau, C.F. Lichti, P. Lindenbaum, F. Charpentier, J.M. Nerbonne, R.R. Townsend, J. Merot, Mass spectrometry-based identification of native cardiac Nav1.5 channel alpha subunit phosphorylation sites, J. Proteome Res. 11 (2012) 5994–6007.
[9] P. Beltran-Alvarez, S. Pagans, R. Brugada, The cardiac sodium channel is post-translationally modified by arginine methylation, J. Proteome Res. 10 (2011) 3712–3719.
[10] P. Beltran-Alvarez, A. Espejo, R. Schmauder, C. Beltran, R. Mrowka, T. Linke, M. Batlle, F. Perez-Villa, G.J. Perez, F.S. Scornik, K. Benndorf, S. Pagans, T. Zimmer, R. Brugada, Protein arginine methyl transferases-3 and -5 increase cell surface expression of cardiac sodium channel, FEBS Lett. 587 (2013) 3159–3165.
[11] S.A. Cohen, L.K. Levitt, Partial characterization of the rH1 sodium channel protein from rat heart using subtype-specific antibodies, Circ. Res. 73 (1993) 735–742.
[12] P.J. Stocker, E.S. Bennett, Differential sialylation modulates voltage-gated Na + channel gating throughout the developing myocardium, J. Gen. Physiol. 127 (2006) 253–265.
[13] Y. Zhang, H.A. Hartmann, J. Satin, Glycosylation influences voltage-dependent gating of cardiac and skeletal muscle sodium channels, J. Membr. Biol. 171 (1999) 195–207.
[14] J.W. Schmidt, W.A. Catterall, Palmitylation, sulfation, and glycosylation of the α subunit of the sodium channel. Role of post-translational modifications in channel assembly, J. Biol. Chem. 262 (1987) 13713–13723.
[15] R.H. Roberts, R.L. Barchi, The voltage-sensitive sodium channel from rabbit skeletal muscle. Chemical characterization of subunits, J. Biol. Chem. 262 (1987) 2298–2303.
[16] E.S. Bennett, Isoform-specific effects of sialic acid on voltage-dependent Na^+ channel gating: functional sialic acids are localized to the S5–S6 loop of domain I, J. Physiol. 538 (2002) 675–690.
[17] J.A. Miller, W.S. Agnew, S.R. Levinson, Principal glycopeptide of the tetrodotoxin/saxitoxin binding protein from Electrophorus electricus: isolation and partial chemical and physical characterization, Biochemistry 22 (1983) 462–470.
[18] L. Tyrrell, M. Renganathan, S.D. Dib-Hajj, S.G. Waxman, Glycosylation alters steady-state inactivation of sodium channel Nav1.9/NaN in dorsal root ganglion neurons and is developmentally regulated, J. Neurosci. 21 (2001) 9629–9637.
[19] E. Bennett, M.S. Urcan, S.S. Tinkle, A.G. Koszowski, S.R. Levinson, Contribution of sialic acid to the voltage dependence of sodium channel gating. A possible electrostatic mechanism, J. Gen. Physiol. 109 (1997) 327–343.
[20] A.R. Ednie, K.K. Horton, J. Wu, E.S. Bennett, Expression of the sialyltransferase, ST3Gal4, impacts cardiac voltage-gated sodium channel activity, refractory period and ventricular conduction, J. Mol. Cell. Cardiol. 59 (2013) 117–127.
[21] C.J. Laedermann, N. Syam, M. Pertin, I. Decosterd, H. Abriel, beta1- and beta3-voltage-gated sodium channel subunits modulate cell surface expression and glycosylation of Nav1.7 in HEK293 cells, Front. Cell. Neurosci. 7 (2013) 137.
[22] J. Zhu, J. Yan, W.B. Thornhill, N-glycosylation promotes the cell surface expression of Kv1.3 potassium channels, FEBS J. 279 (2012) 2632–2644.

[23] T.A. Cartwright, M.J. Corey, R.A. Schwalbe, Complex oligosaccharides are N-linked to Kv3 voltage-gated K+ channels in rat brain, Biochim. Biophys. Acta 1770 (2007) 666–671.
[24] N. Weiss, S.A. Black, C. Bladen, L. Chen, G.W. Zamponi, Surface expression and function of Cav3.2 T-type calcium channels are controlled by asparagine-linked glycosylation, Pflugers Arch. 465 (2013) 1159–1170.
[25] I. Watanabe, J. Zhu, J.J. Sutachan, A. Gottschalk, E. Recio-Pinto, W.B. Thornhill, The glycosylation state of Kv1.2 potassium channels affects trafficking, gating, and simulated action potentials, Brain Res. 1144 (2007) 1–18.
[26] J. Napp, F. Monje, W. Stuhmer, L.A. Pardo, Glycosylation of Eag1 (Kv10.1) potassium channels: intracellular trafficking and functional consequences, J. Biol. Chem. 280 (2005) 29506–29512.
[27] T. Pambrun, A. Mercier, A. Chatelier, S. Patri, J.J. Schott, S.S. Le, M. Chahine, B. Degand, P. Bois, Myotonic dystrophy type 1 mimics and exacerbates Brugada phenotype induced by Nav1.5 sodium channel loss of function mutation, Heart Rhythm. 11 (8) (2014) 1393–1400.
[28] L. Nunez, A. Barana, I. Amoros, M.G. de la Fuente, P. Dolz-Gaiton, R. Gomez, I. Rodriguez-Garcia, I. Mosquera, L. Monserrat, E. Delpon, R. Caballero, A. Castro-Beiras, J. Tamargo, p.D1690N Nav1.5 rescues p.G1748D mutation gating defects in a compound heterozygous Brugada syndrome patient, Heart Rhythm. 10 (2013) 264–272.
[29] D.I. Keller, J.S. Rougier, J.P. Kucera, N. Benammar, V. Fressart, P. Guicheney, A. Madle, M. Fromer, J. Schlapfer, H. Abriel, Brugada syndrome and fever: genetic and molecular characterization of patients carrying *SCN5A* mutations, Cardiovasc. Res. 67 (2005) 510–519.
[30] J. Clatot, A. Ziyadeh-Isleem, S. Maugenre, I. Denjoy, H. Liu, G. Dilanian, S.N. Hatem, I. Deschenes, A. Coulombe, P. Guicheney, N. Neyroud, Dominant-negative effect of SCN5A N-terminal mutations through the interaction of Na(v)1.5 alpha-subunits, Cardiovasc. Res. 96 (2012) 53–63.
[31] A. Mercier, R. Clement, T. Harnois, N. Bourmeyster, J.F. Faivre, I. Findlay, M. Chahine, P. Bois, A. Chatelier, The beta1-subunit of Na(v)1.5 cardiac sodium channel is required for a dominant negative effect through alpha–alpha interaction, PLoS ONE 7 (2012) e48690.
[32] G. Baroudi, V. Pouliot, I. Denjoy, P. Guicheney, A. Shrier, M. Chahine, Novel mechanism for Brugada syndrome: defective surface localization of an *SCN5A* mutant (R1432G), Circ. Res. 88 (2001) E78–E83.
[33] A. Chatelier, A. Mercier, B. Tremblier, O. Theriault, M. Moubarak, N. Benamer, P. Corbi, P. Bois, M. Chahine, J.F. Faivre, A distinct de novo expression of Nav1.5 sodium channels in human atrial fibroblasts differentiated into myofibroblasts, J. Physiol. 590 (2012) 4307–4319.
[34] R. Guinamard, A. Chatelier, M. Demion, D. Potreau, S. Patri, M. Rahmati, P. Bois, Functional characterization of a Ca(2+)-activated non-selective cation channel in human atrial cardiomyocytes, J. Physiol. 558 (2004) 75–83.
[35] A. El Chemaly, C. Magaud, S. Patri, C. Jayle, R. Guinamard, P. Bois, The heart rate-lowering agent ivabradine inhibits the pacemaker current I(f) in human atrial myocytes, J. Cardiovasc. Electrophysiol. 18 (2007) 1190–1196.
[36] I. Deschenes, G. Baroudi, M. Berthet, I. Barde, T. Chalvidan, I. Denjoy, P. Guicheney, M. Chahine, Electrophysiological characterization of SCN5A mutations causing long QT (E1784K) and Brugada (R1512W and R1432G) syndromes, Cardiovasc. Res. 46 (2000) 55–65.
[37] M.E. Gellens, A.L. George Jr., L.Q. Chen, M. Chahine, R. Horn, R.L. Barchi, R.G. Kallen, Primary structure and functional expression of the human cardiac tetrodotoxin-insensitive voltage-dependent sodium channel, Proc. Natl. Acad. Sci. U. S. A. 89 (1992) 554–558.
[38] N. Blom, T. Sicheritz-Ponten, R. Gupta, S. Gammeltoft, S. Brunak, Prediction of post-translational glycosylation and phosphorylation of proteins from the amino acid sequence, Proteomics 4 (2004) 1633–1649.
[39] A. Heifetz, R.W. Keenan, A.D. Elbein, Mechanism of action of tunicamycin on the UDP-GlcNAc:dolichyl-phosphate Glc-NAc-1-phosphate transferase, Biochemistry 18 (1979) 2186–2192.
[40] J. Lippincott-Schwartz, L.C. Yuan, J.S. Bonifacino, R.D. Klausner, Rapid redistribution of Golgi proteins into the ER in cells treated with brefeldin A: evidence for membrane cycling from Golgi to ER, Cell 56 (1989) 801–813.
[41] M. Hoshi, X.X. Du, K. Shinlapawittayatorn, H. Liu, S. Chai, X. Wan, E. Ficker, I. Deschenes, Brugada syndrome disease phenotype explained in apparently benign sodium channel mutations, Circ. Cardiovasc. Genet. 7 (2014) 123–131.
[42] S. Namadurai, D. Balasuriya, R. Rajappa, M. Wiemhofer, K. Stott, J. Klingauf, J.M. Edwardson, D.Y. Chirgadze, A.P. Jackson, Crystal structure and molecular imaging of the Nav channel beta3 subunit indicates a trimeric assembly, J. Biol. Chem. 289 (2014) 10797–10811.
[43] J. Roth, C. Zuber, S. Park, I. Jang, Y. Lee, K.G. Kysela, V. Le Fourn, R. Santimaria, B. Guhl, J.W. Cho, Protein N-glycosylation, protein folding, and protein quality control, Mol. Cells 30 (2010) 497–506.
[44] N.B. Cronin, A. O'Reilly, H. Duclohier, B.A. Wallace, Effects of deglycosylation of sodium channels on their structure and function, Biochemistry 44 (2005) 441–449.
[45] C.J. Waechter, J.W. Schmidt, W.A. Catterall, Glycosylation is required for maintenance of functional sodium channels in neuroblastoma cells, J. Biol. Chem. 258 (1983) 5117–5123.
[46] E.C. Arakel, S. Brandenburg, K. Uchida, H. Zhang, Y.W. Lin, T. Kohl, B. Schrul, M.S. Sulkin, I.R. Efimov, C.G. Nichols, S.E. Lehnart, B. Schwappach, Tuning the electrical properties of the heart by differential trafficking of KATP ion channel complexes, J. Cell Sci. 127 (2014) 2106–2119.
[47] H.Y. Gee, S.H. Noh, B.L. Tang, K.H. Kim, M.G. Lee, Rescue of DeltaF508-CFTR trafficking via a GRASP-dependent unconventional secretion pathway, Cell 146 (2011) 746–760.
[48] B. Hasdemir, D.J. Fitzgerald, I.A. Prior, A.V. Tepikin, R.D. Burgoyne, Traffic of Kv4 K+ channels mediated by KChIP1 is via a novel post-ER vesicular pathway, J. Cell Biol. 171 (2005) 459–469.
[49] J.S. Yoo, B.D. Moyer, S. Bannykh, H.M. Yoo, J.R. Riordan, W.E. Balch, Non-conventional trafficking of the cystic fibrosis transmembrane conductance regulator through the early secretory pathway, J. Biol. Chem. 277 (2002) 11401–11409.